International Journal of Innovative Technology and Exploring Engineering (IJITEE)
ISSN: 2278-3075 (Online), Volume-9 Issue-4, February 2020

Non-Linear Scour Calculator of Skewed Piers

M. A. Nassar

Abstract: ***This paper investigates the impact of skewed piers and their geometrical shape on the scouring. A non-linear equation estimating scour depths around skewed piers (i.e. Piers Scour Calculator PSC) is established experimentally. The rectangular, semicircle and curvilinear piers are investigated. PSC Eq. gives reasonable values compared to formulas of Froechlich (1988), Chitale (1962), Ahmad (1962) and Inglis-Poona (1949). RSQ values equal 92.5%, 83.5% of the training and validating data, respectively. PSC results are convenient with measurements compared to equations of (Richardson & Davis, 2001) and (Melville & Sutherland, 1988). The experimental results showed that values of the scouring parameter d_s/y_3 increase by 200%, 270% and 238% for the rectangular, the semicircle, and the curvilinear piers, respectively as the skewed angle increases from 0^o to 16.7^o. Two empirical equations presenting flow angles and shape factors are developed.***

Keywords: skewed, scour, erosion, equation and piers.

I. INTRODUCTION

Numerous formulas were presented to approximate scouring around piers. Richardson & Davis [16] identified (CSU) equation of erosions. Arneson et al., [1] presented an equation for the skewed angle factor. Shen, et al., (1969) and Inglis (1949) as written by Mueller & Wagner [12] identified two formulas of scouring. Melville and Sutherland [10] gave a detailed design equation of piers' scouring. Mueller et al., [13] evaluated 13- scouring equations. Gaudio et al. [7] accomplished a sensitivity analysis for 6- equations. Beg [2] discovered that Jain & Fischer and Laursen & Toch yield a more realistic guess of erosion depth.

Sheppard, et al. [19] assessed 23-equations of scouring. Padmini, et al. [15] investigated scouring under different flow conditions. Beg and Beg [3] gave a comprehensive revision of reduction methods of scouring. Koustuv and Susanta [8] reported experiments on erosion processes at three piers. Ettema, et al. [5] discussed parameters that affected the skewed factor. Sanoussi and Habib [17] discussed the upstream pier slope and skewed angles.

Mashahir et al., [9] discussed the impact of riprap and the combination between riprap and collar on scouring. Shatirah Akib, et al. [18] investigated the impacts of many parameters in cases of skewed piers.

Revised Manuscript Received on February 28, 2020.
***** Correspondence Author
M. A. Nassar *, Associate professor, Dep. of Construction Eng., College of Eng. in Al-Qunfudhah, Umm Al-Qura University, KSA, on leave from Water Eng. and Water Structures Dep., Faculty of Eng., Zagazig University, Egypt, email: manassar@uqu.edu.sa.

Deshmukh and Raikar [4] indicated that, scouring expanded by the time to the equilibrium value.

Tabarestani and Zarrati [20] proposed a technique to define the riprap dimensions. Nasser [14] applied ANN technique to estimate piers' scour. Fahmy and Nassar [6] showed that existing of specified piles upstream the abutment yielded minimum velocities near piers. Melville and Chiew [11] determined that 50:80% of the equilibrium downward distance of scour was attended at 10% of the time of the equilibrium depth.

This work investigates the impact of skewed piers and the geometrical shape on scouring. Design rules are indicated.

II. THEORETICAL WORK

The scour depends on parameters related to soil, flow & geometric parameters, see Fig. (1). Factors are correlated in Eq. (1). It is modified to Eq. (2). Finally, it is simplified to Eq. (3).

$$f(d_s, y_3, \alpha, L, C_n, \rho, \mu, g, v, a, d_{50}) = 0 \quad (1)$$

$$d_s/y_3 = f(1/R_n, F_3, d_{50}/y_3, \alpha, a/y_3, L/y_3, C_n) \quad (2)$$

$$d_s/y_3 = f(F_3, C_4, C_\alpha, C_{a/L}, C_n) \quad (3)$$

Where: ds is a downward distance of the scouring; y_3 is DS depth of the flow; α is an angle of skewness and L is the pier's extent; C_n is the parameter of the nose type; ρ & μ are the density and viscosity of water, respectively, g is the gravity, d_s/y_3 is the scouring parameter, R_n is Reynolds's number, $F_3 = v/\sqrt{gy_3}$ is the downstream Froude parameter, v is the velocity; d_{50}/y_3 is the parameter of mean size of particles; a/y_3 and L/y_3 are the width and length parameters, respectively. C_4 is a correction coefficient (C_4=1.0 for d_{50} < 2mm, Richardson & Davis [16]), C_α is a coefficient of skewed angle, $C_{a/L}$ is a coefficient of the geometric relation.

III. INSTALLATION OF LAB MODELS

Wooded models are built-in hydraulics lab at the faculty of Eng., Zagazig Univ., Egypt. a flume of 400cm length, 20cm depth and 40cm width is used, see figure (1). Discharges are measured by an orifice meter. Soil and flow depths are measured by a scaled pointer. A 6cm thickness of sandy soil is used [d_{50}=1.8mm]. The adopted time for the test = 60 minutes.

Two series of measurements were applied. The first discovered the impact of α= 0.0^o, 5.75^o, 11.35^o and 16.7^o for three piers on scouring; see table (1) and figures (2 & 3). The second series discovered the impact of geometrical ratio a/L = 0.1, .0175 and 0.25, see figure (3).

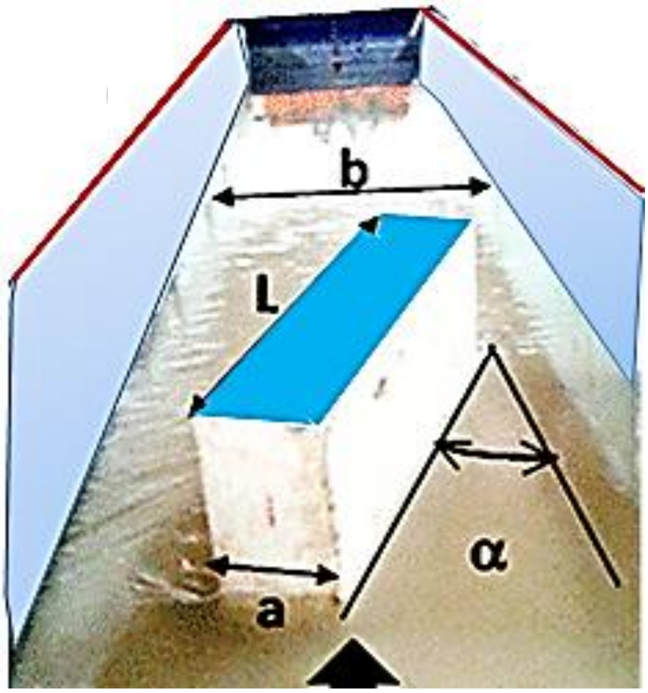

Fig. 1. a photo of the model

IV. FIRST SERIES RESULTS

Figures 4A, 5A and 6A present correlation between d_s/y_3 and F_3 for cases of a rectangular, semicircle and curvilinear piers, respectively. d_s/y_3 values increased by 200, 270 and 238% as {α} increased from α= 0^o to 16.7^o, for rectangular, semicircle, and curvilinear piers, respectively. Figs. 4B, 5B and 6B present relevance between d_s/y_3 and{α}. Values of d_s/y_3 become deeper as {α} increases for different piers. Figure (7) shows scouring patterns for semicircle piers for α= 0^o, 5.75^o, 11.35^o and 16.7^o. $F_3 \cong 0.172$. It clears that, boosting of skewed angle magnifies scouring and decreases symmetry of hole.

Figures 8A and 8B present a correlation between d_s/y_3 and F_3 for a/L =0.175 and 0.25, respectively. The rectangular gives deepest scour depths. Figure (9) shows scour patterns for different noses. The rectangle magnifies values comparing others, while curvilinear reduces the area.

Table- I: Geometric parameters of piers

Rectangle Pier Noses	*Semicircle Pier Noses*	*Curvilinear Pier Noses*
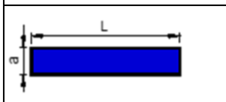	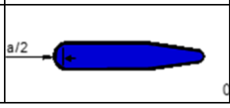	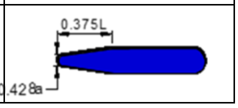

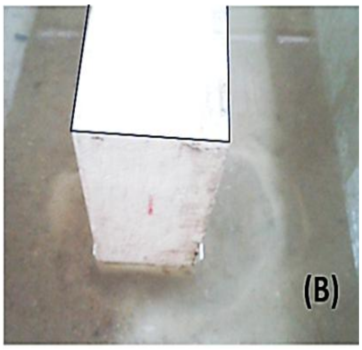

Fig. 2. Scouring photos for rectangular piers [A] α= 16.7^o [B] α= 0^o

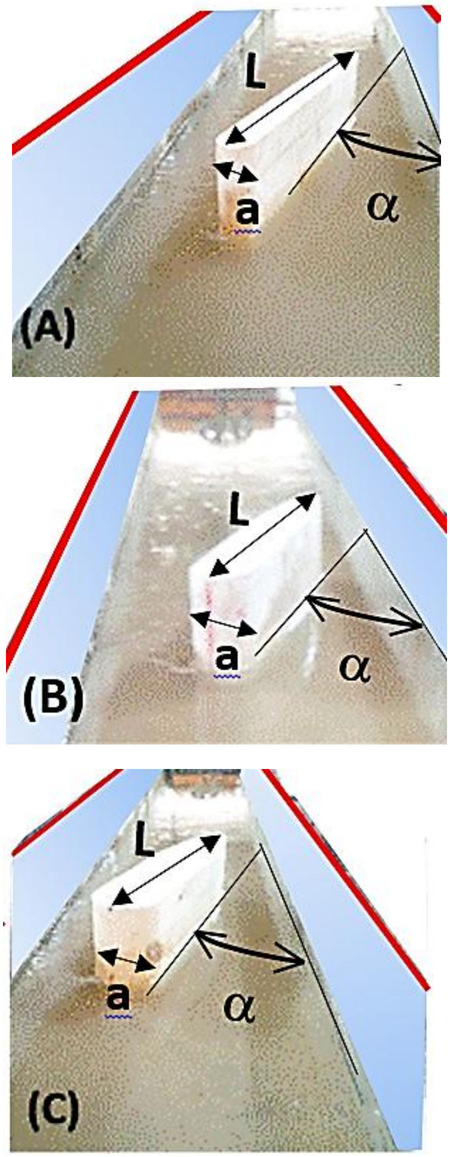

Fig. 3.Selected photos for different geometric ratios of semicircle piers [A] a/L =0.10 [B] a/L =0.175 [C] a/L =0.25

International Journal of Innovative Technology and Exploring Engineering (IJITEE)
ISSN: 2278-3075 (Online), Volume-9 Issue-4, February 2020

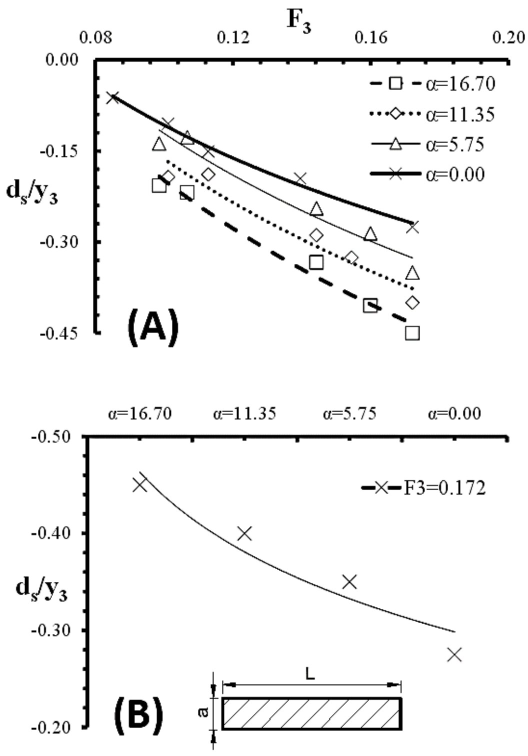

Fig. 4. Cases of rectangular piers of a/L =0.175 [A] d_s/y_3 against F_3 [B] d_s/y_3 against α for F_3 =0.172

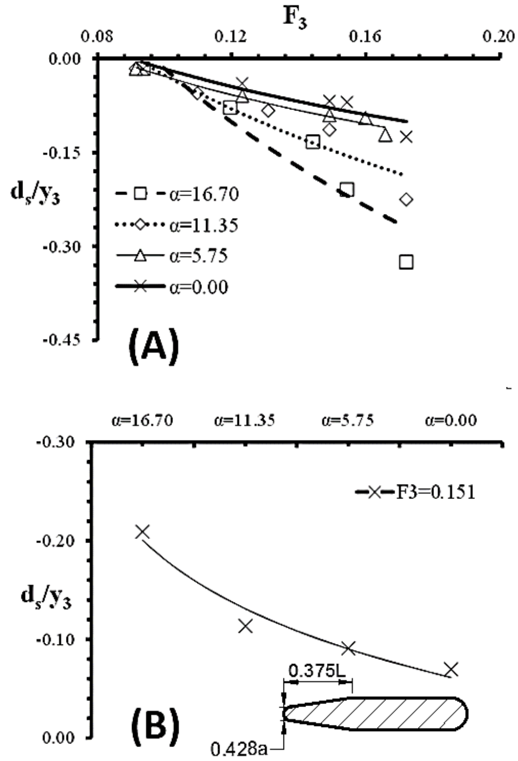

Fig. 6.Cases of curvilinear nose of a/L =0.175 [A] d_s/y_3 against F_3 [B] d_s/y_3 against α for $F_3 \cong$ 0.151

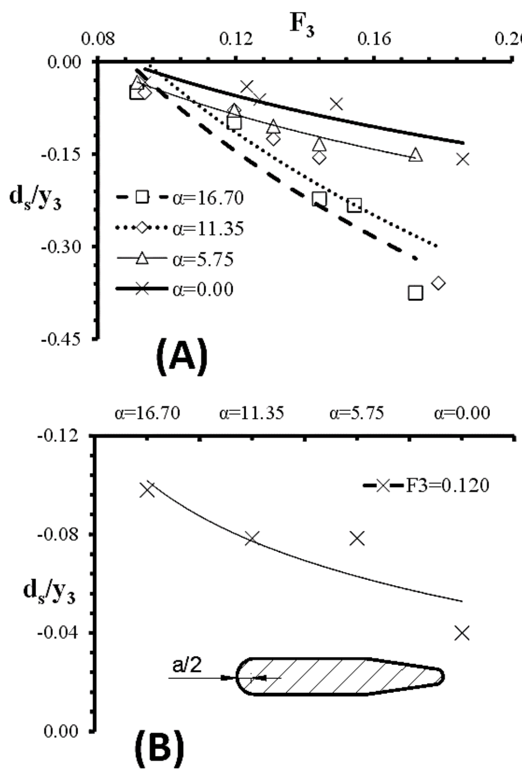

Fig. 5.Cases of semicircle noses of a/L =0.175 [A] d_s/y_3 against F_3 [B] d_s/y_3 against α for $F_3 \cong$ 0.12

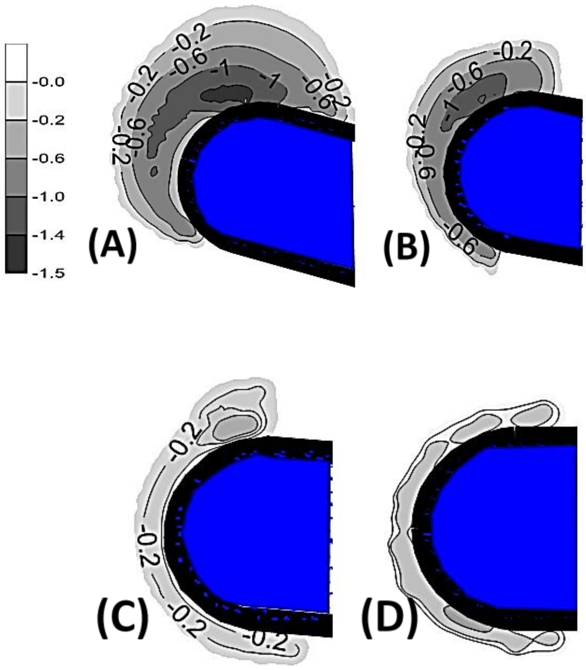

Fig. 7. Scouring patterns for the semicircle nose for different skew angles and a/L =0.175 [A] α= 16.7° and F_3 = 0.172 [B] α= 11.35° and F_3 = 0.178 [C] α= 5.75° and F_3 = 0.172 [D] α= 0° and F_3 = 0.185

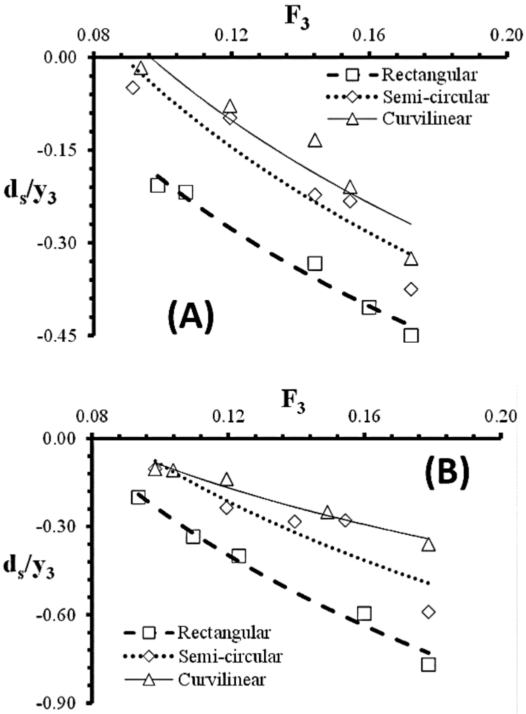

Fig. 8.Relationships of d_s/y_3 against F_3 for different noses [A] α= 16.7° and a/L =0.175 [B] α= 16.7° and a/L =0.25

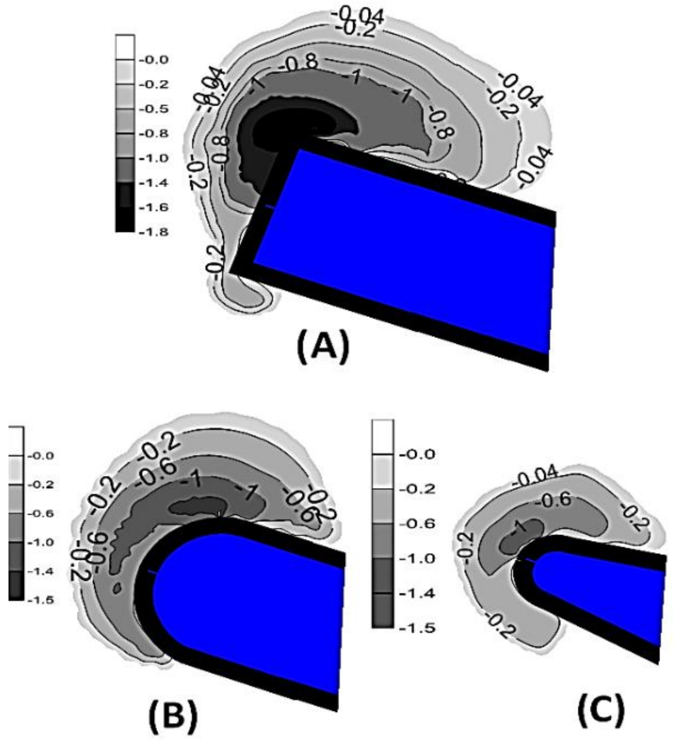

Fig. 9.Scouring patterns for pier noses of α= 16.7°, F_3 = 0.172and a/L =0.175 [A] the rectangle [B] the semicircle [C] the curvilinear

V. SECOND SERIES RESULTS

Figures 10A, 11A and 12A present the correlation between d_s/y_3 and F_3 for a/L =0.1, 0.175, and 0.25 and α= 16.7° for the rectangle, semicircle and curvilinear noses. d_s/y_3 values increases by 168%, 177% and 174% as {a/L } increases from a/L = 0.1 to 0.25, for the rectangular, semicircle, and curvilinear noses, respectively. Figures 10B, 11B and 12B present the relevance between d_s/y_3 and {a/L } for different noses. The nose of {a/L } =0.25gives largest d_s/y_3 values for

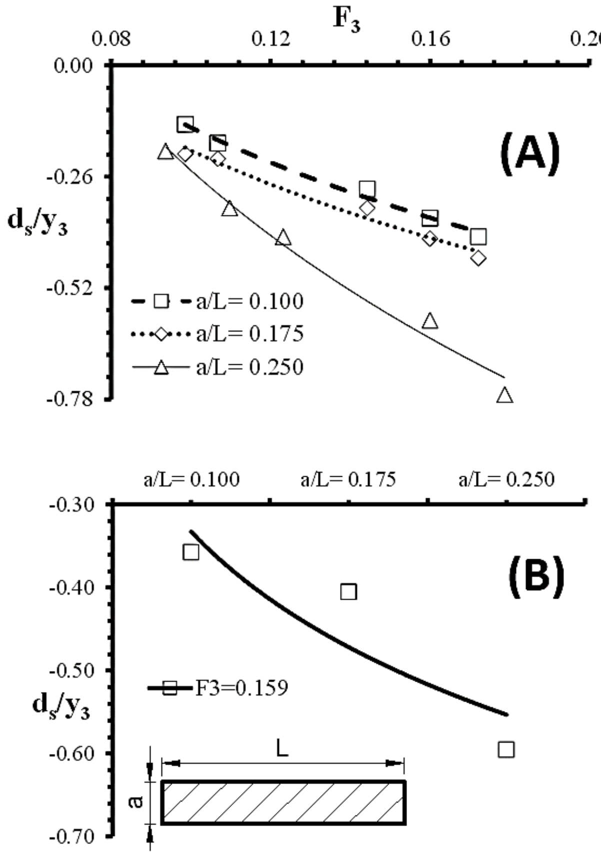

Fig. 10. [A] Relationships of d_s/y_3 against F_3 for α=16.7° [B] Relationships of d_s/y_3 against a/L for $F_3 \cong 0.159$ and α=16.7°

VI. PROPOSED PARAMETERS

C_α and $C_{a/L}$ are adopted as Eqs. (4 and 5), respectively. Constants of equations are given as table (2). Figures 13A and 14A are comparing between measures of C_α and $C_{a/L}$ versus the statistical ones. Figures 13B and 14B are comparing statistical values using Eqs. 4 and 5) and residuals. RSQ for the Eqs. (4 and 5) extend within (66.66%: 90.7%). C_α and $C_{a/L}$values are displayed in Fig. 15.

$$C_\alpha = CO_1 + CO_2 \times \sin(\propto) \qquad (4)$$

$$C_{a/L} = CO_3 + CO_4 \times \frac{a}{L} \qquad (5)$$

Table- II: Parameters of Eqs. (4 and 5)

	Eq. (4)				*Eq. (5)*			
	CO_1	CO_2	*RSQ*	*St. error*	CO_3	CO_4	*RSQ*	*St. error*
Rectangle	0.92	3.11	0.82	0.16	0.35	4.19	0.90	0.12
Semicircle	0.97	5.71	0.93	0.17	0.19	5.07	0.85	0.20
Curvilinear	0.95	4.91	0.66	0.38	0.42	3.59	0.78	0.11

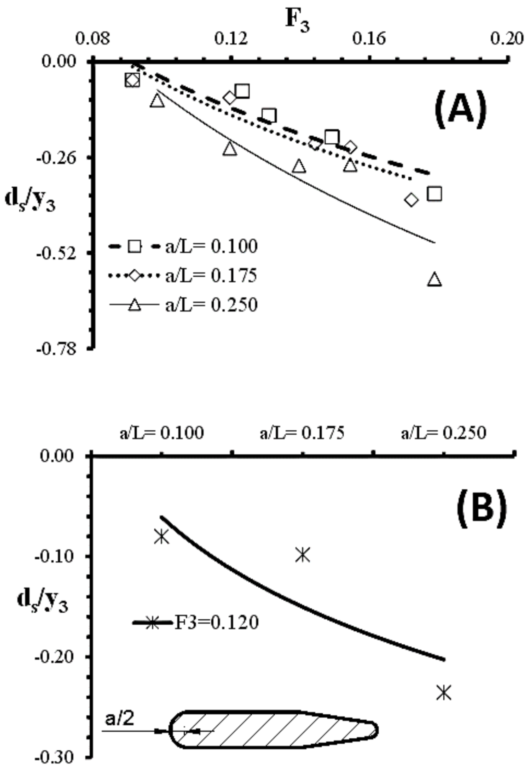

Fig. 11. [A]Relationships of d_s/y_3 against F_3 for α=16.7^o [B] Relationships of d_s/y_3 against a/L for $F_3 \cong 0.12$ and α=16.7^o

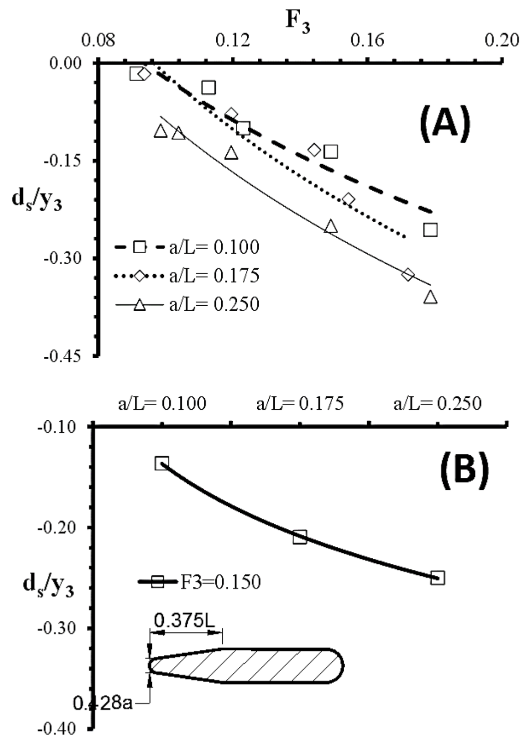

Fig. 12. [A] Relationships between d_s/y_3 against F_3 in case of α=16.7^o and [B] against between d_s/y_3 against a/L for $F_3 \cong 0.15$ and α=16.7^o

VII. PIERS SCOUR CALCULATOR (PSC)

The non-linear regression is applied to establish the equation. Measurements are divided into two main categories, the first is 77.2% used to establish the form, see Eq. (6). 22.8% is applied to confirm the equation. The constants are tabulated in the table (3). The minimal values of RSQ = 92%, 83% for the training and confirmation, respectively. Figure 16B is comparing between collected and the detected d_s/y_3 by Eq. (6). Figure 16A presents a comparing between calculations by Eq. (6) and residuals. There is a clear random allocation. Eq. (6) is applied for {α} = 0^o: 16.7^o, F_3 = 0.085: 0.185 and a/L = 0.1: 0.25.

$$d_s/y_3 = \mathrm{x}\, C_{a/L}{}^{x1}\, C_{\propto}{}^{x2}\, F_3{}^{x3} \qquad (6)$$

VIII. CALIBRATION OF PSC

PSC Eq. is reformulated in comparable format to the other known equations as $\{d_s/y_1\}$. Figures 17 and 18 shows a comparing between d_s/y_1, (i.e. $[y_3/y_1 \times$ outputs of PSC Eq.]), Froechlich (1988), Chitale (1962), Ahmad (1962) and Inglis-Poona (1949) using the confirmation data. Figures 17A and 17B presents d_s/y_1 via F_1 for (α= 16.7^o & a/L =0.175) and (α= 16.7^o & a/L =0.25), respectively. Figures 18A and 18B presents d_s/y_1 via F_1 for (α= 16.7^o & a/L =0.175) and (α= 16.7^o & a/L =0.25), respectively.

PSC Eq. gives the most fitted line with experiments. Figures 19 and 20 compare between RMSE for different equations in cases of the rectangle and semicircle noses, respectively. PSC Eq. gives the minimal values of RMSE. PSC Eq. is compared to Richardson & Davis (2001) and Melville & Sutherland (1988) equations, see figures 21 and 22 for the rectangle and semicircle cases, respectively. PSC Eq. Values are very close to the confirmation data. The other equations exceed results of PSC Eq. by about 850%.

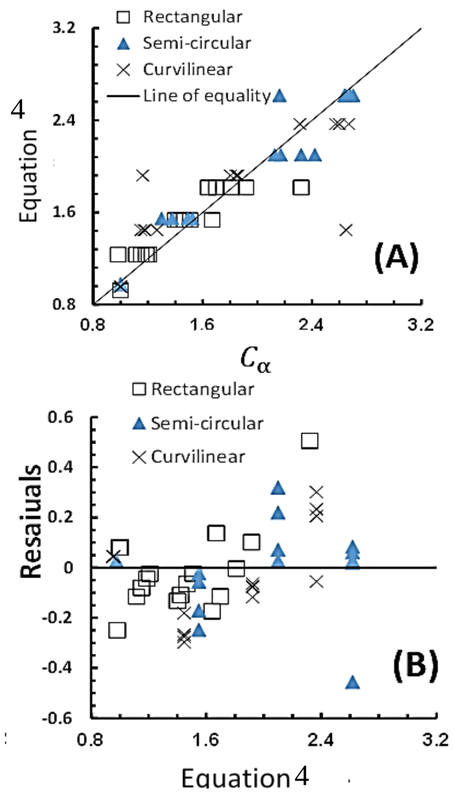

Fig. 13. [A] Eq. 4 against lab values [B] Eq. 4 against residuals

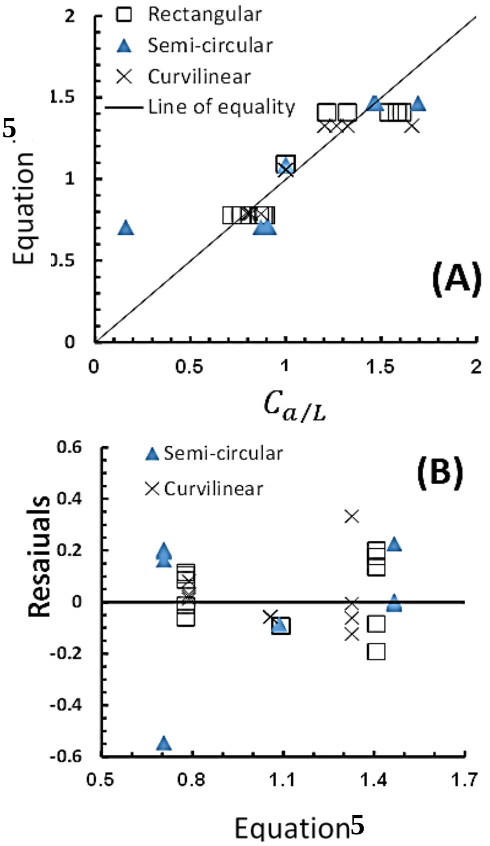

Fig. 14. [A] Eq. 5 against lab values [B] Eq. 5 against residuals

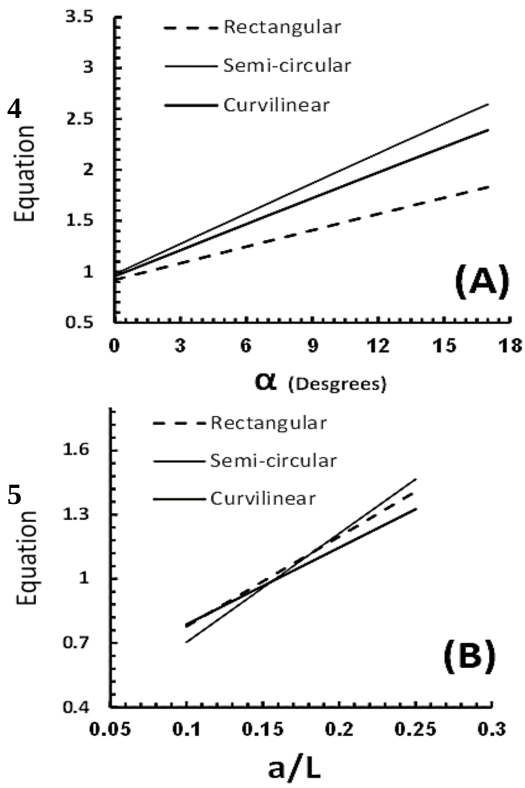

Fig. 15. [A] C_{α} for different {α} [B] $C_{a/L}$ for different {a/L }

Table- III: Parameters of Eq. (12)

	Confirm. Data		*Training Data*		x	$x1$	$x2$	$x3$
	RSQ	RMSE	RSQ	RMSE				
Rectangle	0.83	0.06	0.92	0.04	-6.517	0.682	0.834	1.819
Semicircle	0.83	0.02	0.93	0.02	-6.185	0.563	1.705	2.583
Curvilinear	0.89	0.03	0.93	0.04	-9.329	0.907	1.453	2.734

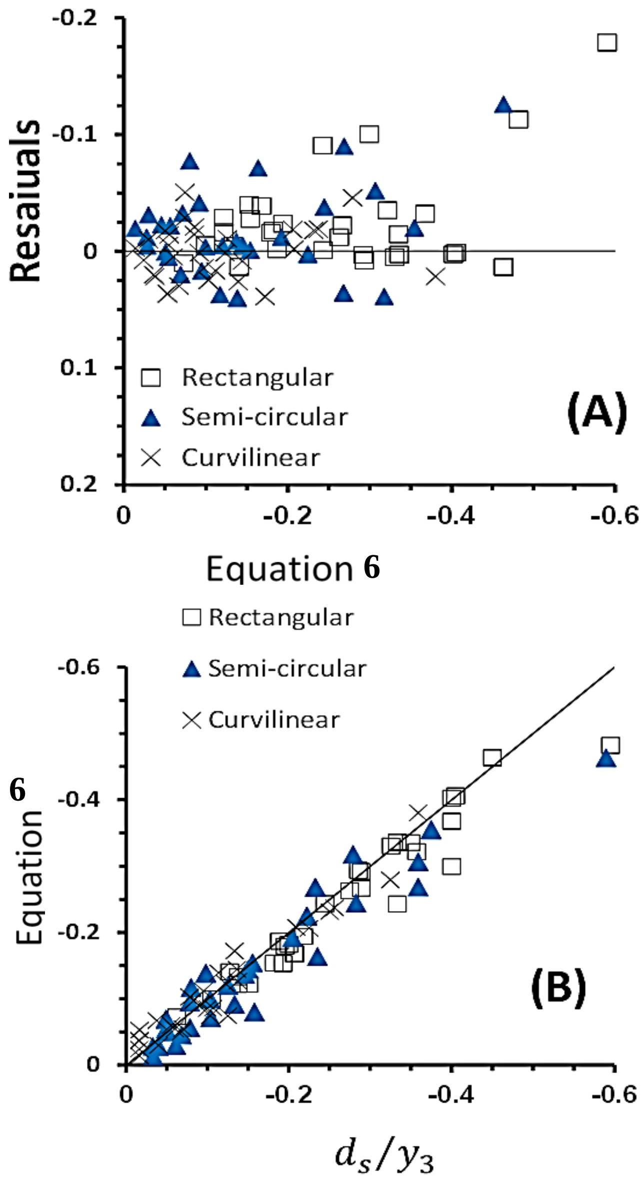

Fig. 16. [A] Eq. (6) against residuals [B] Eq. (6) against lab values

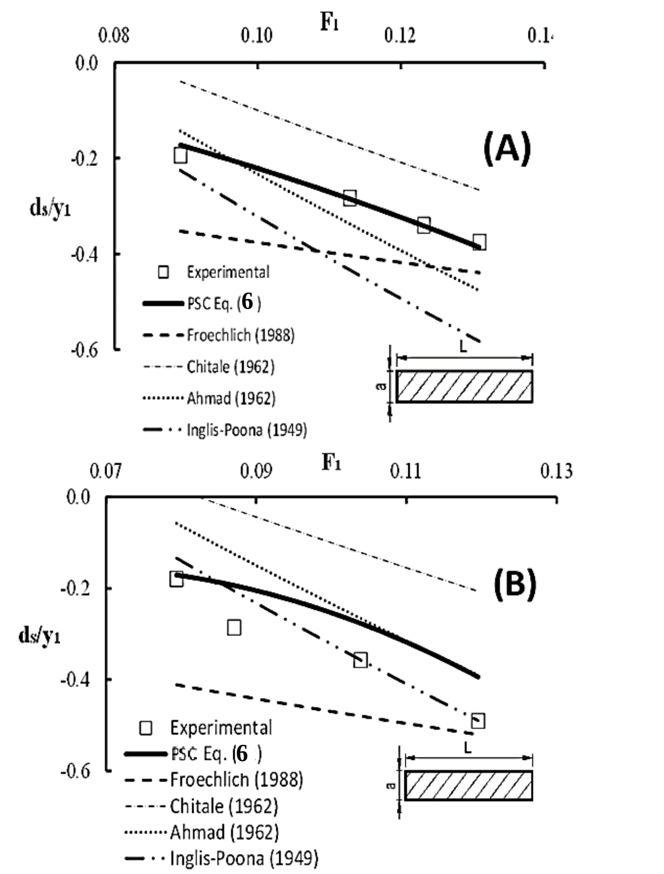

Fig. 17. Relationships between d_s/y_1 against F_1 [A] α= 16.7° and a/L =0.175 [B] α= 16.7° and a/L =0.25

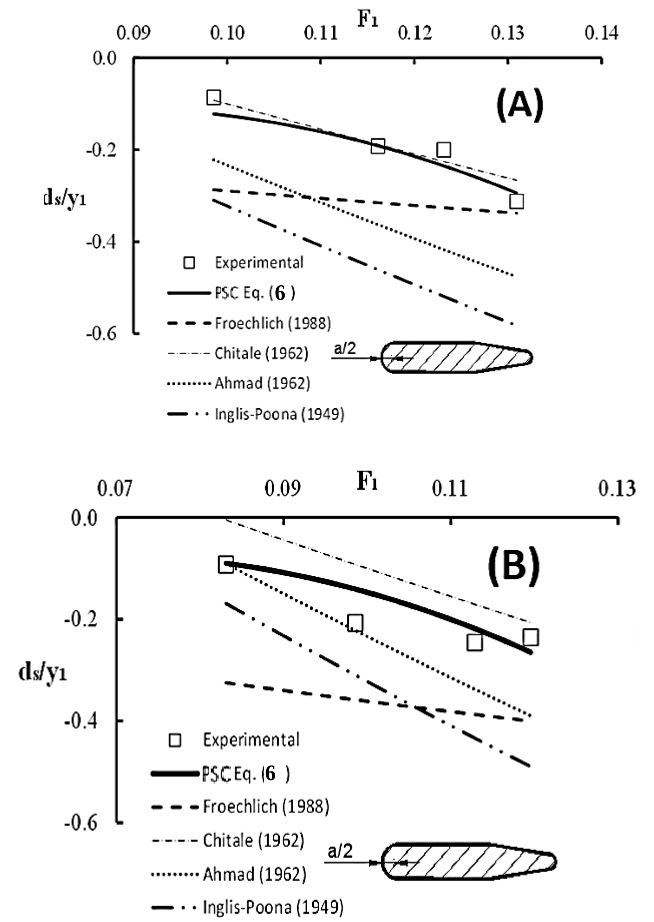

Fig. 18. Relationships between d_s/y_1 against F_1 [A] α= 16.7° and a/L =0.175 [B] α= 16.7° and a/L =0.25

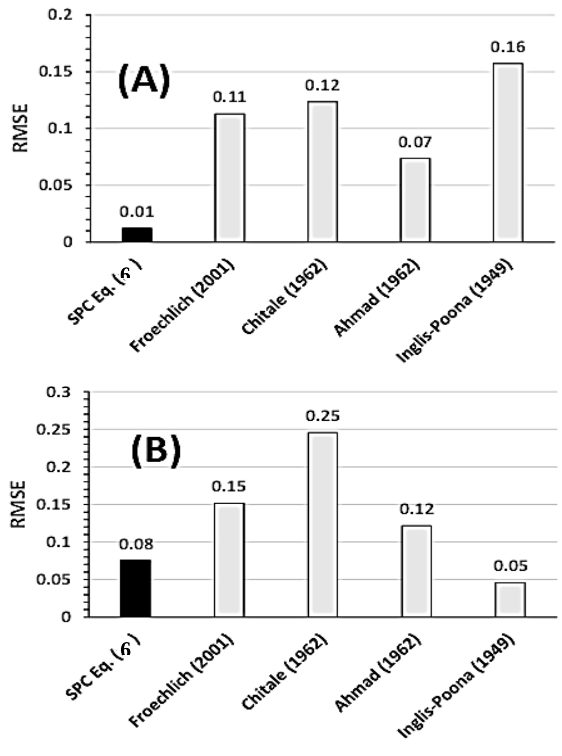

Fig. 19. RMSE for different equations for the rectangular pier [A] α= 16.7° and a/L =0.175 [B] α= 16.7° and a/L =0.25

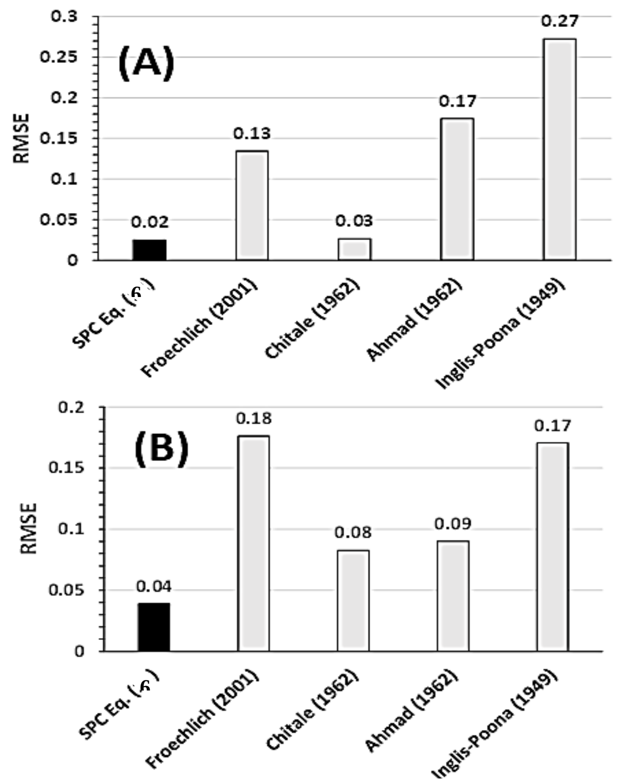

Fig. 20. RMSE for different equations for semicircle pier [A] α= 16.7° and a/L =0.175 [B] α= 16.7° and a/L =0.25

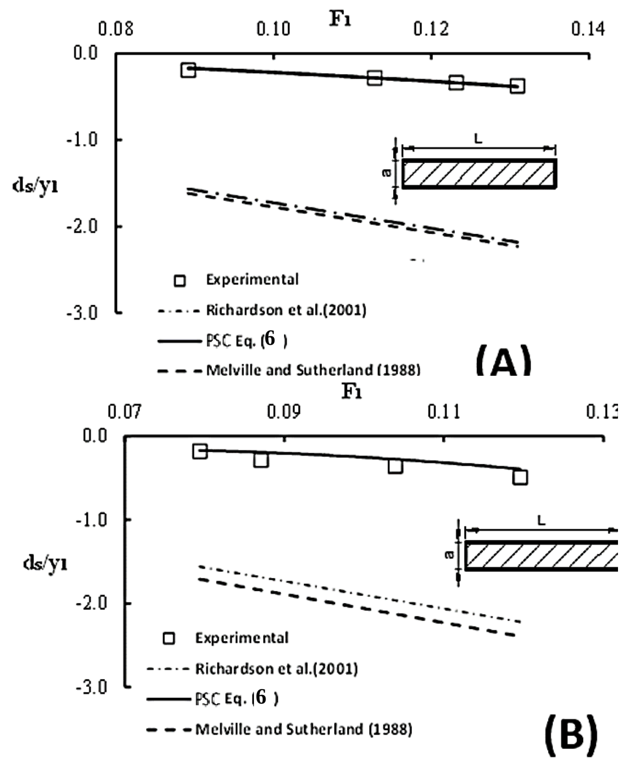

Fig. 21. Relationships between d_s/y_1 against F_1 for rectangular pier nose [A] α= 16.7^o and a/L =0.175 [B] α= 16.7^o and a/L =0.25

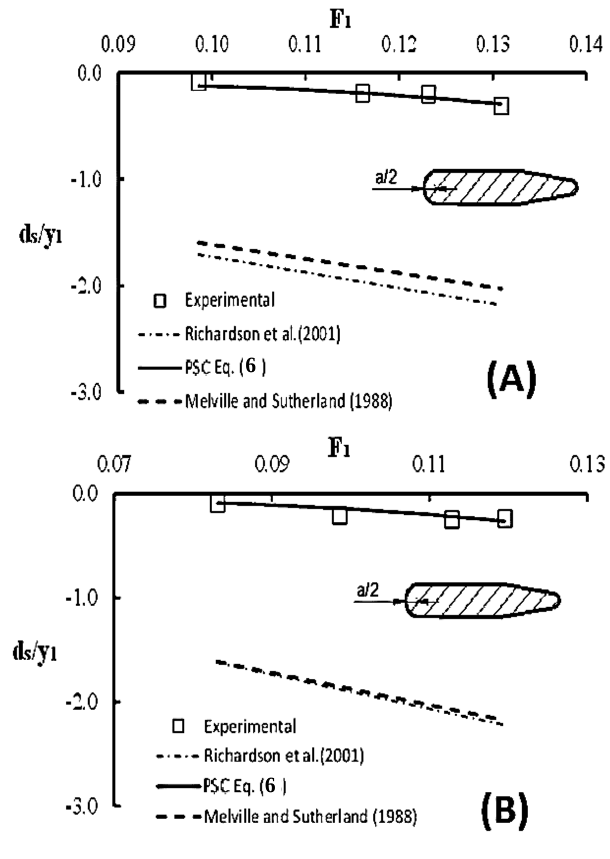

Fig. 22. Relationships between d_s/y_1 against F_1 for semicircle pier nose [A] α= 16.7^o and a/L =0.175 [B] α= 16.7^o and a/L =0.25

IX. CONCLUSIONS

The next conclusions can be listed.

1. d_s/y_3 values increase by 200%, 270% and 238% as the skewed angle {α} increases from α= 0^o to 16.7^o for the rectangular, the semicircle, and the curvilinear, respectively.
2. The rectangular nose gives deepest d_s/y_3.
3. d_s/y_3 values increase by 168%, 177% and 174% as $\{a/L\}$ increases from 0.1 to 0.25, for the rectangular, the semicircle, and the curvilinear piers, respectively.
4. Two equations of C_α and $C_{a/L}$ are generated. RSQ for the equations extend within (66.66% to 90.7%).
5. PSC Eq. has a minimal RSQ of 92% and 83% for the training and confirmation data, respectively.
6. PSC Eq. is evaluated compared to Chitale (1962), Froechlich (1988), Ahmad (1962) and Inglis-Poona (1949). PSC Eq. gives the minimal values of RMSE.
7. PSC Eq. is evaluated compared to equations of (Richardson & Davis, 2001) and Melville & Sutherland (1988). The results of the two equations exceed the results of PSC Eq. by 850%.

REFERENCES

1. Arneson L.A., Zevenbergen L.W., Lagasse P.F., Clopper P.E., (2012), "EVALUATING SCOUR AT BRIDGES", Fifth Edition, Publication No. FHWA-HIF-12-003, HEC-18, U.S. Department of Transportation, Federal Highway Administration, the National Technical Information Service, Springfield, VA 22161 (703) 487-4650.
2. Beg M. (2013), "Predictive competence of Existing Bridge Pier Scour Depth Predictors", European Inter. Journal of Science and Technology, Vol. 2 No. 1.
3. Beg M. and Beg S., (2013), "Scour Reduction around Bridge Piers: A Review", International Journal of Engineering Inventions e-ISSN: 2278-7461, p-ISSN: 2319-6491 Volume 2, Issue 7 (May 2013) PP: 07-15. www.ijeijournal.com.
4. Deshmukh A. R. and Raikar R. V. (2014), "A Clear Water Scour Around a Circular Bridge Pier Under Steady Flow for Different Opening Ratios", IJRET: International Journal of Research in Engineering and Technology eISSN: 2319-1163, pISSN: 2321-7308. Volume: 03 Issue: 01, http://www.ijret.org.
5. Ettema, R., Mostafa, E., Melville, B., and Yassin, A. (1998). "Local Scour at Skewed Piers." J. Hydraul. Eng., 124(7), 756–759. doi.org/10.1061/(ASCE)0733-9429(1998)124:7(756).
6. Fahmy M R. and Nassar M. A., (2017), "Contraction effect upstream abutments on velocity and scour: experimental and theoretical study using IRIC software", Journal of Engineering Sciences, Assiut University, Faculty of Engineering, Vol. 45 No. 1, January 2017 PP. 17 – 27.
7. Gaudio R., Tafarojnoruz A. and De Bartolo S., (2013), "Sensitivity analysis of bridge pier scour deptii predictive formulae", Journal Of Hydroinformatics, IWA Publishihg 2013, pp. 939-951, doi: 10.2166/hydro.2013.036.
8. Koustuv Debnath and Susanta Chaudhuri , (2012), "Local scour around non-circular piers in clay–sand mixed cohesive sediment beds", Engineering Geology 151 (2012) 1–14, http://dx.doi.org/10.1016/j.enggeo.2012.09.013.
9. Mashahir, M., Zarrati, A., and Mokallaf, E. (2010). "Application of Riprap and Collar to Prevent Scouring around Rectangular Bridge Piers." J. Hydraul. Eng., 136(3), 183–187. doi.org/10.1061/(ASCE)HY.1943-7900.0000145.
10. Melville B. W. and Sutherland A. J., (1988), "Esign Method for Local Scour At Bridge Piers", J. Hydraul. Eng. Volume 114, Issue 10 (October 1988) pp.1210-1226, doi: 10.1061/(ASCE)0733-9429(1988)114:10(1210).
11. Melville, B. and Chiew, Y. (1999), "Time Scale for Local Scour at Bridge Piers" J. Hydraul. Eng., 125(1), 59–65. doi: 10.1061/(ASCE)0733-9429(1999)125:1(59)
12. Mueller, D. S., & Wagner, C. R. (2005), "Field observations and evaluations of streambed scour at bridges" (No. FHWA-RD-03-052).

13. Mueller D.S., Miller R. L., and Wilson J. T., (1994), "Historical and Potential Scour Around Bridge Piers and Abutments of Selected Stream Crossings in Indiana", U.S. GEOLOGICAL SURVEY, Water-Resources Investigations Report 93-4066. Indianapolis, Indiana.
14. Nasser, M. A. (2008), "Estimation of local scour and energy loss at bridge piers using neural networks", Alex. Eng. Journal, Faculty of Eng., Alex. Univ., Egypt,, 47(4), 339-353.
15. Padmini K., Soumendu S. R., Subhasish D., Rajib D. and Asis M., (2012), "Scour hole characteristics around a vertical pier under clear water scour conditions", ARPN J. of Eng. and Applied Sciences, VOL. 7, NO. 6, pp. 649-654, JUNE 2012.
16. Richardson, E. V., & Davis, S. R. (2001). "Evaluating scour at bridges", Circular No. 18. Report No.FHWA NHI, 01-001.
17. Sanoussi A. A., Habib E. A. (2008), "Local Scour at Rounded and Sloped Face Piers With Skew Angles: Part 1", ICCBT 2008 - D - (41) – pp439-462.
18. Shatirah Akib, Moatasem M. Fayyadh, Ismail Othman, (2011)," Structural Behaviour of a Skewed Integral Bridge Affected by Different Parameters", The Baltic Journal of Road and Bridge Engineering, Vol VI, No 2, p. 107-114, DOI: 10.3846/bjrbe.2011.15.
19. Sheppard, D., Melville, B., and Demir, H. (2014). "Evaluation of Existing Equations for Local Scour at Bridge Piers." J. Hydraul. Eng., 140(1), 14–23. doi.org/10.1061/(ASCE)HY.1943-7900.0000800.
20. Tabarestani, M., & Zarrati, A. R. (2015), "Design of Riprap Stone Around Bridge Piers Using Empirical and Neural Network Method", Civil Engineering Infrastructures Journal, 48(1), 175-188.

AUTHORS PROFILE

M. A. Nassar, Associate professor, Department of Construction Engineering, College of Engineering in Al-Qunfudhah, Umm Al-Qura University, KSA, on leave from Water Engineering and Water Structures Department, Faculty of Engineering, Zagazig University, Egypt, email: manassar@uqu.edu.sa.